Determination of Group Index Using Unbalanced Mach–Zehnder Interferometers

1. Purpose and Scope

The objective is to determine the group index of a 220 nm silicon-on-insulator (SOI) strip waveguide by analyzing the spectral interference fringes of unbalanced Mach–Zehnder interferometers (MZIs).

A set of MZIs with different differential arm lengths was designed in KLayout, simulated using Lumerical INTERCONNECT, and analyzed to extract the free spectral range (FSR) near 1550 nm. The group index was then calculated directly from the extracted FSR and the known path-length imbalance.

In addition, two calibration structures (CAL1 and CAL2) were included to estimate waveguide propagation loss, which provides useful for interpreting fringe visibility and spectral quality.

2. Background and Theory

An MZI splits the input optical field into two arms and recombines them at the output. When the two arms have a length difference ΔL, the relative phase difference varies with wavelength, producing periodic constructive and destructive interference in the transmission spectrum. The phase difference between the two arms is:

$$\Delta\phi(\lambda) = \frac{2\pi}{\lambda}\, n_g(\lambda)\, \Delta L.$$

This produces periodic constructive and destructive interference in the transmission spectrum. The wavelength spacing between adjacent fringes is the free spectral range (FSR). Near a center wavelength λ_0,

$$\mathrm{FSR}(\lambda_0) \approx \frac{\lambda_0^2}{n_g\, \Delta L}, n_g \approx \frac{\lambda_0^2}{\mathrm{FSR}(\lambda_0)\, \Delta L}.$$

Thus, once the FSR is extracted from the spectrum and $\Delta L$is known from the layout, $n_g$follows directly.

3. Device Layout Design

3.1 Platform and Waveguide Geometry

- SOI device layer thickness: 220 nm
- Waveguide type: strip waveguide
- Nominal waveguide width: 500 nm
- Polarization: TE
- Design and layout tool: KLayout (SiEPIC flow)

3.2 MZI Device Set (Primary Group Index Extraction)

Five unbalanced MZIs were designed with increasing differential arm length $\Delta L$to verify the expected inverse scaling of FSR with ΔL.

Table 1. Interferometer naming and path-length difference

Interferometer	ΔL(μm)
MZIA	24
MZIB	29
MZIC	34
MZID	39
MZIE	44

All devices share the same couplers and general routing style; only $\Delta L$is varied. Figure 1 shows schematic of Lumerical INTERCONNECT for unbalanced Mach–Zehnder interferometer MZIA.

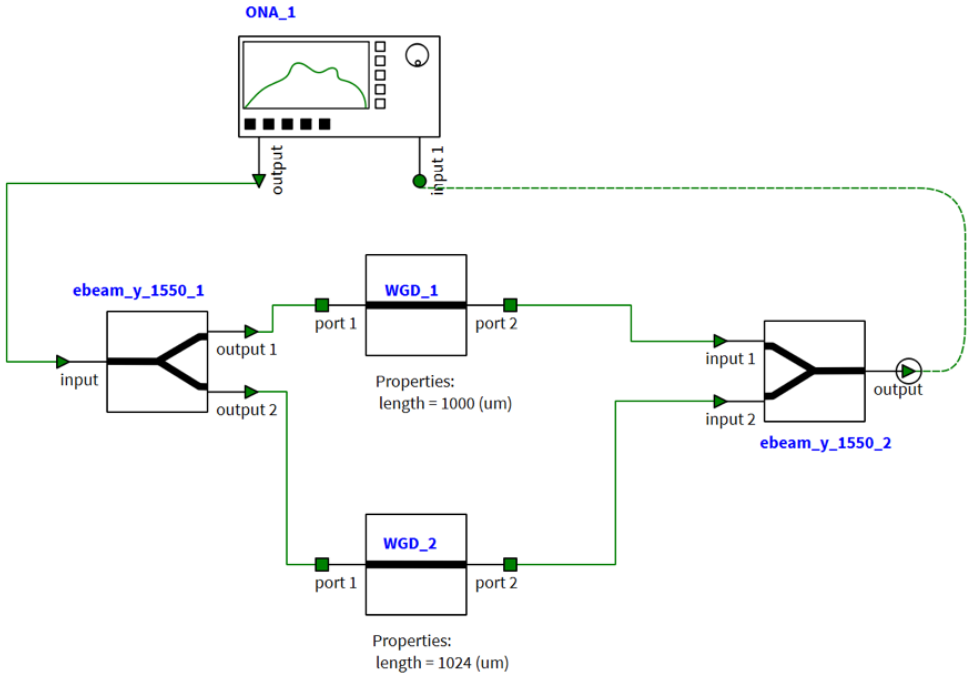

Figure 1. Lumerical INTERCONNECT schematic of the unbalanced Mach–Zehnder interferometer (MZIA) with $\Delta L = 24\ \mu m$ for transmission analysis.

3.3 Additional Structures

- CAL1, CAL2: straight waveguides with identical grating couplers and different waveguide lengths, used to estimate propagation loss.
- MZIAA, MZIAB, MZIAC: additional MZIs with much larger ΔL(200–400 µm) and different routing styles, used to validate group-index extraction over a wide ΔLrange.
- Figure 2 shows layout of the submitted chip block (MZI set + CAL structures)

Figure 2. Layout of the submitted chip block (MZI set + CAL structures)

4. Simulation Workflow

4.1 Tool and Setup

- Simulator: Lumerical INTERCONNECT
- Components:
  - Grating couplers (TE)
  - 2×2 couplers / Y-splitters
  - Waveguide models consistent with the layout
- Wavelength sweep: 1500–1600 nm
- Output metric: TE transmission (reported as TE gain in dB)

4.2 Simulation Outputs

For each device:

- Transmission spectrum $T(\lambda)$
- Identification of interference fringes
- Extraction of FSR near 1550 nm using the same algorithm the same approach typically used for measured spectra.

5. FSR and Group Index Extraction: MZIA to MZI-E

5.1 FSR Extraction Method

From each simulated transmission spectrum, successive deep minima were identified and the spacing between adjacent minima was computed as:

$$\mathrm{FSR} = \lambda_{m+1} - \lambda_m.$$

FSR values were extracted from minima near 1550 nm; when multiple fringe pairs were available, the average spacing was reported.

5.2 Results

Figure 3 shows simulated transmission spectra (TE) versus wavelength for the five Mach–Zehnder interferometers MZIA through MZIE. Each trace shows the interference fringes over the 1500–1600 nm band; the fringe spacing (FSR) decreases as the arm-length imbalance ΔL increases. These spectra are used to extract the FSR and subsequently compute the waveguide group index.

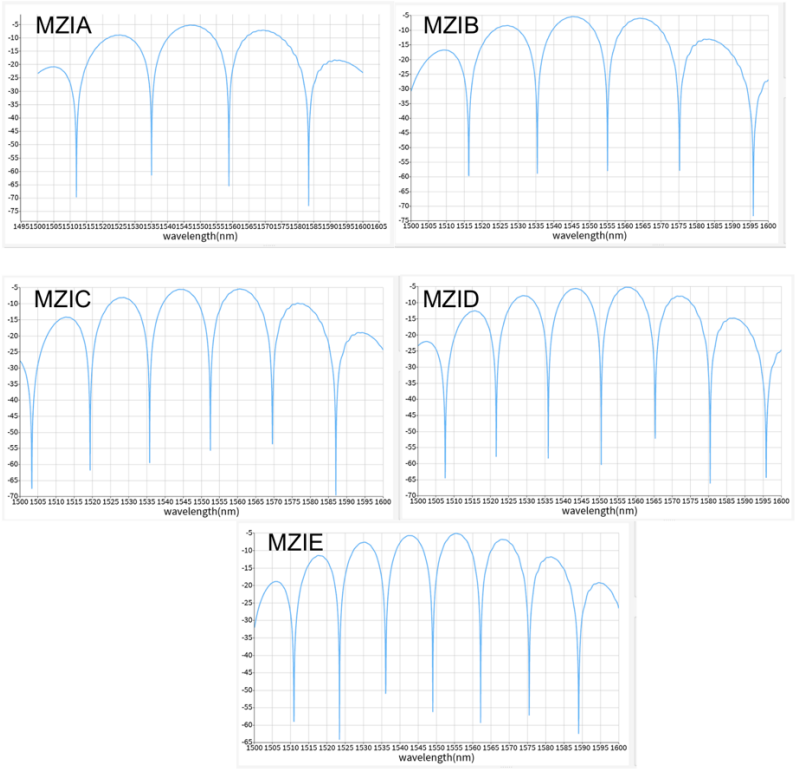

Figure 3. Simulated TE transmission spectra vs. wavelength for MZIA–MZIE (1500–1600 nm).

Table 2. Extracted FSR and group index for MZIA to MZI-E (near 1550 nm)

Device	ΔL(μm)	FSR (nm)	Adjacent fringe pairs used	Extracted n_g
MZIA	24	23.800	1	4.213
MZIB	29	19.640	1	4.214
MZIC	34	16.740	1	4.222
MZID	39	14.705	2	4.190
MZIE	44	13.015	2	4.196

5.3 Discussion

As expected, the FSR decreases monotonically as ΔLincreases, consistent with the designed imbalance. The extracted group index is consistent across the five devices, with $n_g \approx 4.21$near 1550 nm. Small variations are attributed to spectral resolution, local dispersion, and uncertainty in fringe identification.

6. Validation Using Large-ΔL Devices (MZIA, MZIAA, MZIAB, MZIAC)

To further validate the extraction method, four MZIs with much larger path-length differences were analyzed:

Table 3. Large-ΔL validation devices.

Device	ΔL(μm)
MZIA	24
MZIAA	200
MZIAB	300
MZIAC	400

These devices exhibit very dense fringes, allowing averaging over many fringe periods. Figure 4 shows simulated TE transmission spectra for the MZI set used in group-index extraction: baseline MZIA (ΔL = 24 μm) and extended-delay devices MZIAA/AB/AC (ΔL = 200/300/400 μm). The decreasing fringe spacing with increasing ΔL is used to measure FSR and compute n_g.

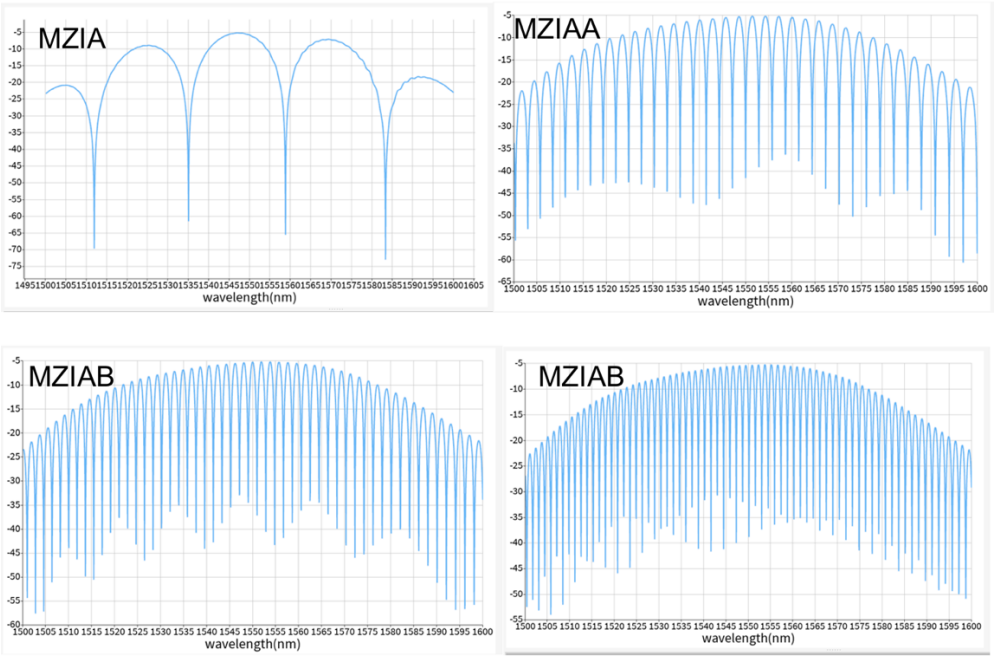

Figure 4. Simulated TE transmission spectra for MZIA and MZIAA/AB/AC.

Table 4 summarizes the extracted FSR and group index from Lumerical simulation.

Table 4. FSR and extracted group index (ΔL sweep)

Device	ΔL(μm)	FSR (nm)	Extracted n_g
MZIA	24	23.800	4.206
MZIAA	200	2.829	4.246
MZIAB	300	1.906	4.202
MZIAC	400	1.427	4.209

The extracted group index is highly consistent across the ΔL sweep (mean $n_g \approx 4.22$), confirming that the observed FSR variation is dominated by the designed path-length difference rather than spectral artifacts.

7. Propagation Loss Estimation Using CAL1 and CAL2

Two calibration waveguides (CAL1 and CAL2) were included to estimate the propagation loss. CAL1 and CAL2 use identical grating couplers and routing style, but differ in waveguide length by:

$$\Delta L_{\mathrm{CAL}} = 100\ \mu\mathrm{m}$$

The simulated transmission is reported in dB (TE gain). Defining CAL2 as the longer waveguide, the wavelength-dependent propagation loss is computed from the differential transmission:

$$\Delta T(\lambda) = T_{\mathrm{CAL2}}(\lambda) - T_{\mathrm{CAL1}}(\lambda),$$

$$\alpha(\lambda) = \frac{\Delta T(\lambda)}{\Delta L_{\mathrm{CAL}}}.$$

Because $\Delta L_{\mathrm{CAL}} = 0.01\ \mathrm{cm}$

this simplifies to:

$$\alpha(\lambda) = 100 \times [T_{\mathrm{CAL2}}(\lambda) - T_{\mathrm{CAL1}}(\lambda)][\mathrm{dB/cm}].$$

Averaging $\alpha(\lambda)$over 1545–1555 nm gives an estimated propagation loss of approximately:

$$\alpha \approx 7\ \mathrm{dB/cm}$$

This estimate is sensitive to residual spectral ripple because the length difference is relatively small; however, it provides a useful consistency check and helps interpret overall spectral quality and fringe visibility in the MZI simulations.

8. Conclusion

A set of unbalanced Mach–Zehnder interferometers (MZIs) was designed, simulated, and analyzed to extract the group index of a 220-nm SOI strip waveguide. The measured/simulated FSR scales inversely with the designed path-length difference, and the extracted group index is consistent across both small- and large-ΔL devices:

$$\boxed{n_g(1550\ \mathrm{nm}) \approx 4.21}$$

The inclusion of calibration waveguides provides additional context on propagation loss and supports the robustness of the group-index extraction.

9. References

- Lukas Chrostowski, Michael Hochberg, *Silicon Photonics Design*, Cambridge University Press, 2015.
- UBC Course/lab notes

10. Acknowledgments

I/We acknowledge the edX UBCx Phot1x Silicon Photonics Design, Fabrication and Data Analysis course, which is supported by the Natural Sciences and Engineering Research Council of Canada (NSERC) Silicon Electronic-Photonic Integrated Circuits (SiEPIC) Program. The devices were fabricated by Richard Bojko at the University of Washington Washington Nanofabrication Facility, part of the National Science Foundation's National Nanotechnology Infrastructure Network (NNIN), and Cameron Horvath at Applied Nanotools, Inc. Mateo Branion-Calles performed the measurements at The University of British Columbia. We acknowledge Lumerical Solutions, Inc., Mathworks, Mentor Graphics, Python, and KLayout for the design software.